Received: 24 December 2023 | *Revised:* 25 April 2024 | *Accepted:* 23 May 2024
DOI: 10.37917/ijeee.22.1.16 *Vol. 22 | Issue 1 | June 2026*

Iraqi Journal for Electrical and Electronic Engineering
Original Article

Open Access
IJEEE University of Basrah College of Engineering

Comparative Analysis of Rectifier Circuits: Performance Evaluation And Efficiency Comparison

Othman Anwar*, Ahmed M A Sabaawi
College of Electronics Engineering, Ninevah University, Mosul, Iraq

Correspondance
*Othman Anwar
College of Electronics Engineering, Ninevah University, Mosul, Iraq
Email: ahmed.sabaawi@uoninevah.edu.iq

Abstract
In this paper, a comparison between different types of rectifier circuits for RF energy harvesting is conducted. Six types of rectifier circuits consisting of half-wave, full-wave, voltage doubler, Villard charge pump, Graetz charge pump, and Dickson charge pump are designed and simulated. These various types of rectifier circuits are designed for different resistance loads, HSMS282X diodes and standard substrate materials that represents the dielectric constant. Firstly, the rectifiers are firstly designed on an FR-4 substrate with a thickness of 1.6 mm and a dielectric constant of 4.3 using a single-stage LC-match method at 2.4 GHz. The studied range of the input power was from 0 dBm to 30 dBm, the resistance load is 3 kΩ, and the HSMS2820 diode is used. The highest recorded output voltage for the Graetz charge pump was around 27 V, while the highest recorded efficiency for the Graetz charge pump was also 27%. Advanced Design System (ADS) software is used to simulate the rectifier circuits..

Keywords
RF Energy Harvesting, Impedance Matching Network (IMN), Rectifier Circuits, Advanced Design System (ADS) Software.

I. Introduction

Not only are fifth-generation (5G) technologies providing the groundwork for a sophisticated, high-performance wireless communication infrastructure, but also they additionally provide possibilities for swift socio-economic growth and the transformation of digital technology. With the advent of 5G technology, there is now greater possibility to connect a number of handheld devices with sensing and communication capabilities and establish a secure, quick connection between them [1].
In the next years, thousand millions of electronic gadgets are predicted to be capable of connection thanks to 5G and Information technology networks [2, 3].
To ensure that these sensor appliances continue to operate sustainably, technicians must continue to provide these devices with perpetual electricity. One option is to use a rectenna system to charge these devices wirelessly, which might also save money by minimizing the need to replace batteries and hard wires. WPT, meaning wireless power transfer and RFEH, meaning radio-frequency energy harvesting offer an alternate means of recharging the sensing components, enabling easy portability and reducing maintenance expenses [4]. The rectifier circuit plays a crucial role in the Rectenna (Rectifying antenna) system. Rectenna systems have attracted a lot of attention from the RF engineering field since they have made a substantial contribution to the actual implementation of RFEH and WPT systems [5, 6].
The literature has extensively researched only a single-band, wide-band and multiple-band rectenna technology for energy harvesting since communication networks employ several frequency bands [7–11].
It is becoming more possible to achieve batteryless function for medicinal applications by collecting energy from sound wave, renewable energy, heating, and radio-frequency (RF) sources [12–15].
When it comes to biomedical devices, RF energy harvesting

is one of these methods that demonstrates the most promise when other sources are insufficient. Additional uses for RF energy harvesting are in Internet of Things applications and the Radio Frequency Identification (RFID) system. Many of these applications take advantage of the widely-used Bluetooth low-energy (BLE) and WiFi connection protocols.

For radio frequency (RF) energy harvesting applications, one of the integrated circuit, or IC, design aims is to create highly efficient energy harvesting circuits throughout a wide input power scale in order to maximize the output power. Often, it also has to sustain the minimum desired input level of power in order to keep the system functioning correctly. New design techniques and analysis for underlying circuit designs have been made possible by those circuits and system design approaches [16–21].

The ideal powering frequency rises as the energy harvester and matching network's sizes decrease [22]. This paper compares the performance of compact single stage rectifiers for ambient RF energy harvesting and shows the tradeoffs so the user can find out the best choice of rectifier circuit based on his own application and conditions. The designed rectifier circuits were simulated using ADS Software. Six different design of rectifier circuits at 2.4 GHz with LC-match circuit are half-wave, full-wave, voltage doubler, Villard charge pump, Graetz charge pump, and Dickson charge pump were designed and simulated.

II. Design a Single Stage Rectifier Circuits

Half-wave, full-wave, voltage doubler, Villard charge pump, Graetz charge pump, and Dickson charge pump design and simulation are carried out at 2.4 GHz, using Advanced Design System (ADS) Software. Wireless Power Transmission (WPT) is a reliable method of transferring power from a source to an end system without the need of cables or connections. This task is performed by rectennas, which are antennas coupled with rectifiers. Undoubtedly, the rectifier, which converts RF power received into DC power, is the most important component of the rectenna. RF energy is taken in by the antenna and transferred to the matching circuit. The antenna and rectifier's impedances will be matched using a LC-matching circuit, while the Schottky diode type HSMS-2820, HSMS-282B and HSMS-282C are utilized for rectification. It is worth mentioning that choosing the right diode is one of the most vital factors. The resistance load (R_L) is vary from 1 kΩ to 5 kΩ. Furthermore, the dielectric constant (ε_r) are selected for several material such as Rogers R04725JXR, Rogers R04534, FR-4, Porcelain, Rogers R03006 and Rubber with a 2.64, 3, 3.55, 4.3, 6 and 6.5, respectively, for comparison purposes

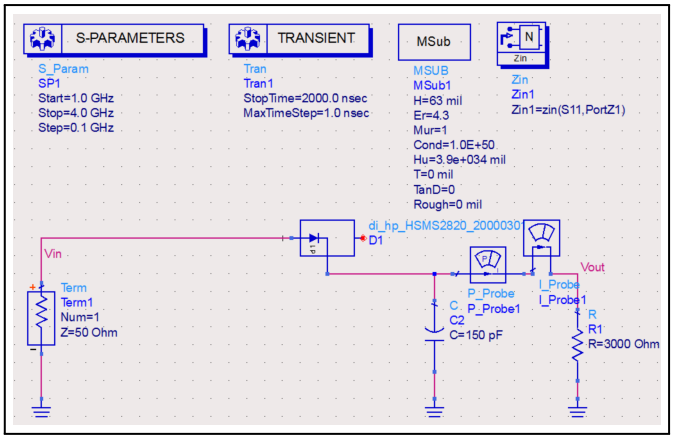

Fig. 1. Simulated circuit to find Zin for half-wave at frequency band 2.4 GHz.

and a thickness of 1.57 mm is used for all six types of rectifier circuits. The simulation results, including DC output voltage (Vout) with respect to the input power and efficiency with respect to the input power at different resistance loads, HSMS-282X diode, and Epsilon of substrate (ε_r), are recorded and plotted at 2.4 GHz frequency band.

A. *Impedance Matching Circuit*

LC (Inductance and Capacitance)-Matching Method is employed in this paper. To find the input impedance (Zin) of the half-wave rectifier circuit, ADS simulations were carried out without any matching network as shown in Fig. 1. The input impedance is plotted over the frequency range of 2.34 GHz to 2.50 GHz, and it is found that Zin at 2.4 GHz is equal to 6.391-j64.235 Ω, as shown in Fig. 2.

Now, to compute the values of L and C of the matching method, use the following equations [23]:

$$Q_s = Q_p = \sqrt{\frac{R_+}{R_-} - 1} \tag{1}$$

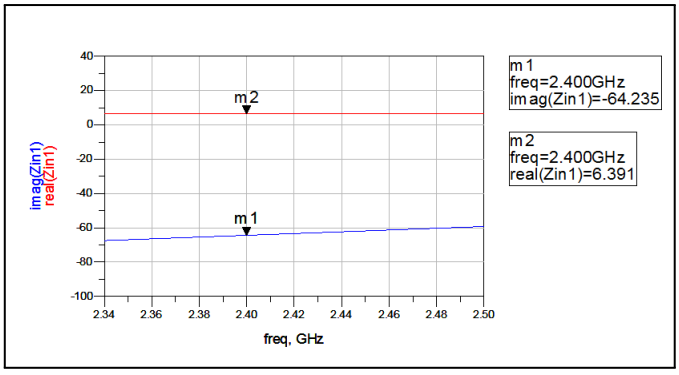

Fig. 2. Simulated value of Zin.

Then:

$$Q_s = \frac{X_s}{R_-} \tag{2}$$

$$Q_p = \frac{R_+}{X_p} \tag{3}$$

Where R_- is the source resistance,
R_+ is the load resistance,
Q_s is the Serial Q Factor and
Q_p is the parallel Q Factor.
From the Eq. 2 and.3, the values of Q_s and Q_p can be calculated to be: $Q_s = Q_p = 2.612$

$Q_s = \frac{X_s}{R - R_4}$
$X_s = 2.612 \times 6.391 = 13.548$
$X_s = X_L = 2\pi fL \rightarrow 2 \times \pi \times 2.4 \times 10^9 \times L$

$$L = \frac{13.548}{2\times\pi\times2.4\times10^9} = 0.89 \text{ nH}$$

$Q_p = \frac{R_+}{X_p}$
$X_p = \frac{50}{2.612} = 19.142$
$X_p = X_C = \frac{1}{2\pi fC} \rightarrow 19.142 = \frac{1}{2\times\pi\times2.4\times10^9\times C}$

$$C = \frac{1}{2\times\pi\times2.4\times10^9\times19.142} = 3.4\ pF$$

The source impedance is pure resistance (50 Ω) with no reactive component; hence, the parallel capacitance will have an additional value of 3.4 pF. Conversely, the series inductor's computed value for the load side is 0.89 nH. On the other hand, it is evident that the load, which is comparable to the rectifier's impedance (6.391-j64.235 Ω), has a reactive portion (+j64.235) that has to be resonated out. An inductor with a value of L=4.41 nH can help achieve this. L=0.89nH+4.41nH=5.3 nH must be the total additional inductor provided to the circuit as a result.

B. Half-wave rectifier circuit

As shown in Fig. 3, a single-stage half-wave rectifier is simulated in the Advanced Design System (ADS). A power source, which in such systems is anticipated as the antenna component, is found in the employed circuit. The power source has an internal impedance of 50 Ω and transmits RF power from 0 to 30 dBm at 2.4 GHz. The matching network circuit for the rectifier circuit, which consists of an LC-circuit, is chosen to match between the antenna and the rectifier. Furthermore, HSMS-2820, HSMS-282B, and HSMS-282C diodes, respectively, were used while keeping the resistance load at 3 kΩ and Epsilon of substrate (ε_r) equals to 4.3, which contributes

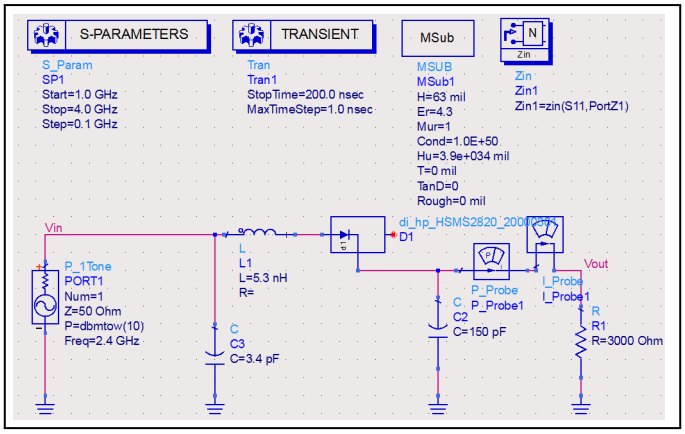

Fig. 3. Half-wave rectifier circuit operating at 2.4 GHz with LC-circuit.

to rectifying the coming RF signal and transforming it from alternating current AC to direct current DC. In the next step, the resistance load is set to 1, 2, 3, 4, and 5 kΩ, respectively, while keeping HSMS2820 diodes and ε_r equal to 4.3. Additionally, the circuit has a smoothing capacitance (C_2) that removes harmonics and smooth the DC power, as illustrated in Fig. 3. In another simulation step, the FR-4 substrate was replaced another substrates having a dielectric constant of 2.64, 3, 3.55, 4.3, 6, and 6.5 that are set in the ε_r MSub block and a thickness of 1.6 mm that is set in the H MSub block, where 63 mil equals to 1.6 mm. The matching network has done the job perfectly, where excellent matching is achieved, as shown in the S-parameters curve in Fig. 4.

Fig. 5 displays the input voltage waveform that is fed to the half-wave rectifier circuit in the 2.4 GHz frequency band with an LC-circuit, which is simulated by ADS Software.

Fig. 6 illustrates the output voltage waveform for a half-wave rectifier circuit at 2.4 GHz. The achieved DC output voltage is around 1.2 V, as shown in Fig. 6.

Fig. 7 displays the waveform of output current for the half-wave rectifier circuit at 2.4 GHz. The output current is

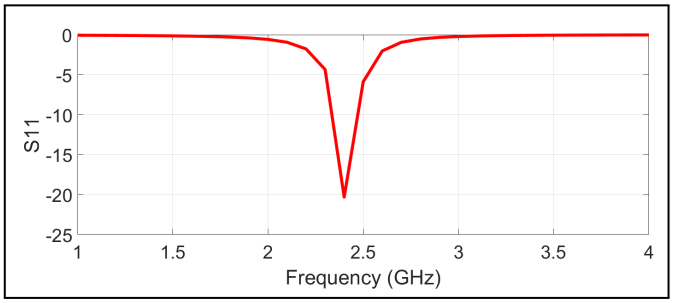

Fig. 4. Simulated S11 of half-wave rectifier circuit at 2.4 GHz with LC-circuit.

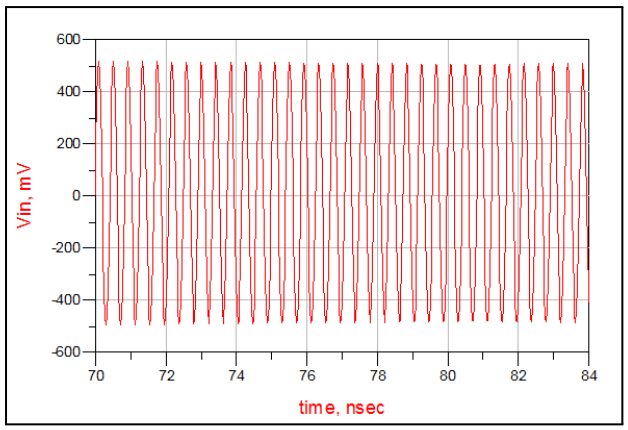

Fig. 5. Vin (V) of half-wave rectifier circuit at 2.4 GHz with LC-circuit.

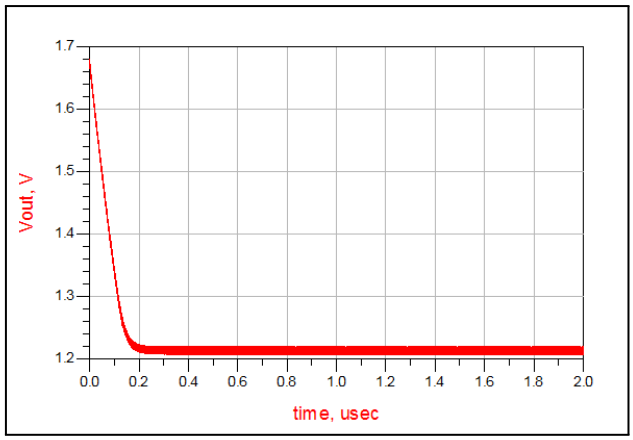

Fig. 6. Vout (V) of half-wave rectifier circuit at 2.4 GHz with LC-circuit.

about 400 μA.

Fig. 8 shows the comparison in Vout of the rectifier's performance when changing the resistance load from 1 to 5 kΩ with a step of 1 kΩ. It has been investigated that there is little impact on the Vout at low input power (Pin) on the contrary at high input power (Pin).

Fig. 9 shows the comparison in Vout of the rectifier's performance when changing diodes, where HSMS2820, HSMS282B, and HSMS282C diodes are used, respectively. It has been discovered that diodes have little effect on Vout.

Fig. 10 shows the comparison in Vout of the rectifier's performance when changing in ε_r, where 2.64, 3, 3.55, 4.3, 6, and 6.5 are utilized, respectively. It is seen that there is no

Fig. 11 shows the comparison in efficiency (η) of the rectifier's performance when changing the load resistance from 1 to 5 kΩ. It has been found that the efficiency (η) decreases with an increasing (R_L).

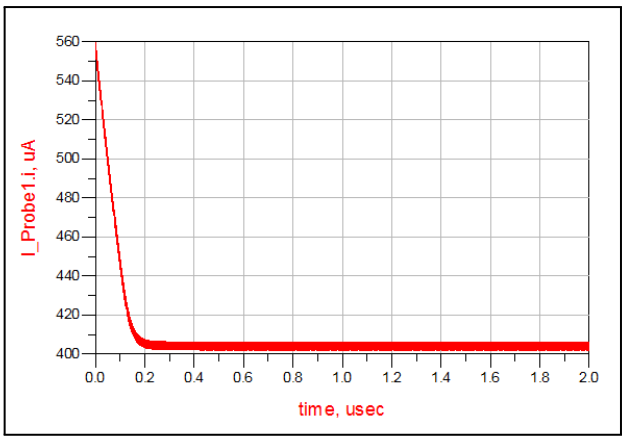

Fig. 7. Output current of half-wave rectifier circuit at 2.4 GHz with LC-circuit.

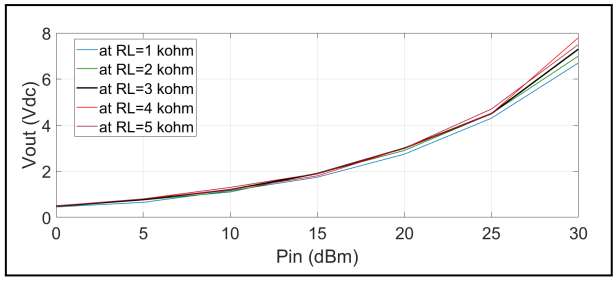

Fig. 8. Vout versus Pin of half-wave rectifier circuit for different resistance values of load (R_L) at 2.4 GHz with LC-circuit.

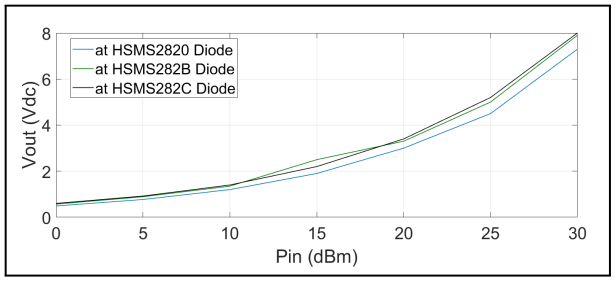

Fig. 9. Vout (V) versus Pin (dBm) of Half-wave rectifier circuit for different Diodes at 2.4 GHz with LC-circuit

Fig. 12 shows the comparison in efficiency (η) of the rectifier's performance when changing diodes. It has been investigated that the best efficiency (η) was with the use of HSMS282C Diode.

Fig. 13 shows the comparison in efficiency (η) of the rectifier's performance when changes in ε_r are made, respectively. It has been investigated that there is little impact on the efficiency (η) at high input power (Pin) on the contrary at low input power (Pin).

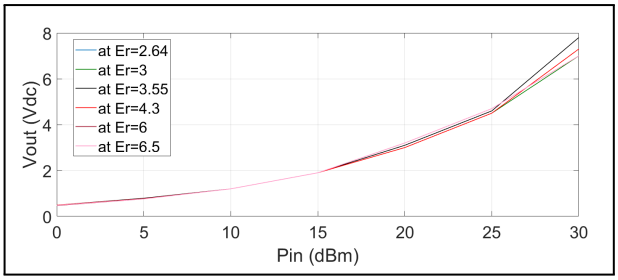

Fig. 10. Vout (V) versus Pin (dBm) of half-wave rectifier circuit for different ε_r at 2.4 GHz with LC-circuit.

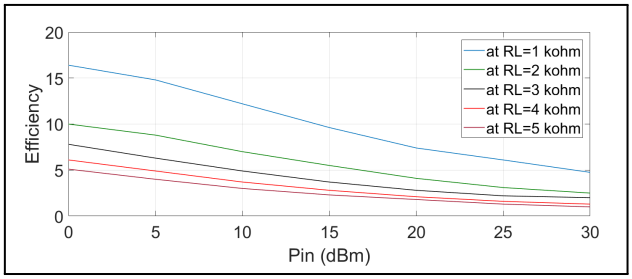

Fig. 11. Efficiency (η) versus Pin (dBm) of half-wave rectifier circuit for different values of resistance load (R_L) at 2.4 GHz with LC-circuit.

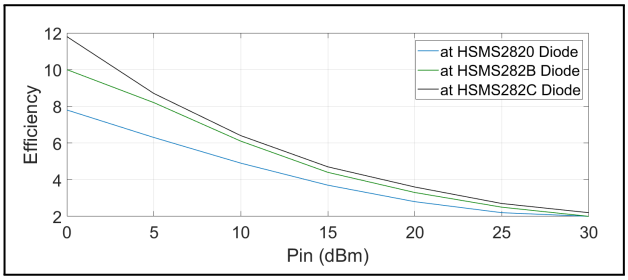

Fig. 12. Efficiency (η) versus Pin (dBm) of half-wave rectifier circuit for different Diodes at 2.4 GHz with LC-circuit.

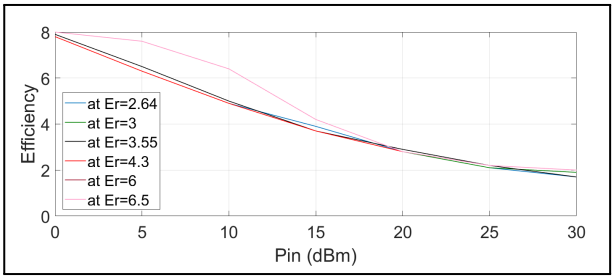

Fig. 13. Efficiency (η) versus Pin (dBm) of half-wave rectifier circuit for different ε_r at 2.4 GHz with LC-circuit.

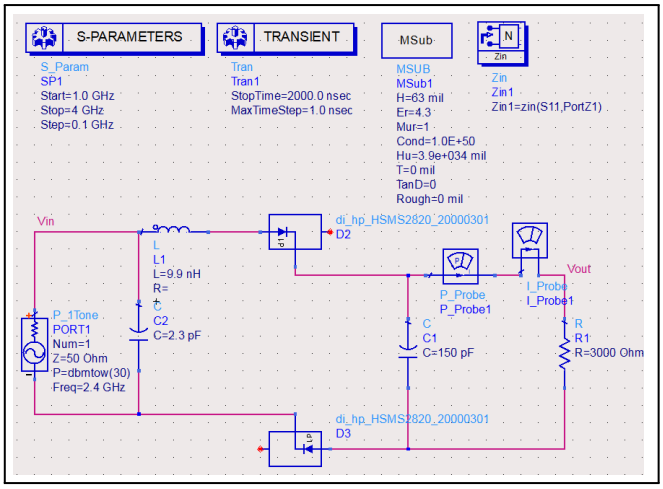

Fig. 14. Full-wave rectifier circuit operating at 2.4 GHz with LC-circuit.

C. *Full-wave rectifier circuit*

Another rectifier circuit is applied by using the full-wave. In this way, an inductance (L) and capacitance (C) are employed at the input part of the circuit to match the source to the rectifier circuit as illustrated in Fig. 14. Fig. 15 shows the simulated S11 of full-wave rectifier circuit at 2.4 GHz with LC-circuit, where the return loss value went below -34 dB.

Fig. 16 shows the comparison in Vout of the rectifier's performance when changing the resistance load from 1 to 5 kΩ with a step of 1 kΩ. It has been noticed that there is little impact on the Vout at low input power (Pin) on the contrary at high input power (Pin).

Fig. 17 shows the comparison in Vout of the rectifier's performance when changing diodes, where HSMS2820, HSMS282B, and HSMS282C diodes are used, respectively. It has been discovered that the diode HSMS2820 exhibits better performance compared to other types

Fig. 18 shows the comparison in Vout of the rectifier's performance when changing in ε_r, where 2.64, 3, 3.55, 4.3, 6, and 6.5 are used, respectively. It has been noted that there is

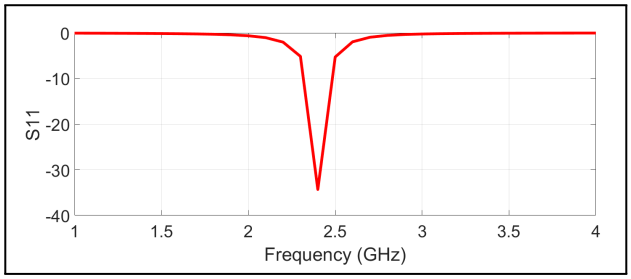

Fig. 15. Simulated S11 of full-wave rectifier circuit at 2.4 GHz with LC-circuit.

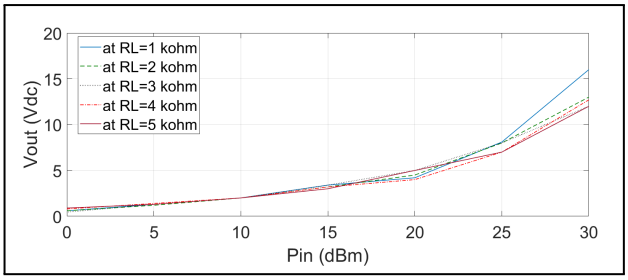

Fig. 16. Vout (V) versus Pin (dBm) of full-wave rectifier circuit for different resistance load (R_L) at 2.4 GHz with LC-circuit.

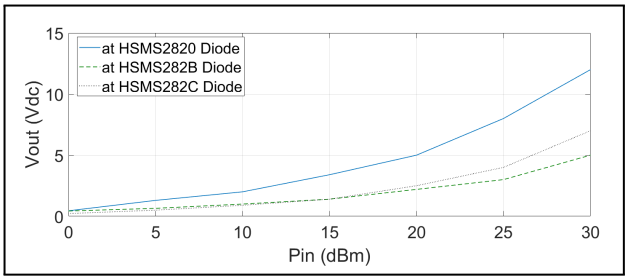

Fig. 17. Vout (V) versus Pin (dBm) of full-wave rectifier circuit for different diodes at 2.4 GHz with LC-circuit.

no impact on the Vout at low input power (Pin) and high input power (Pin), but there is a difference when using a value of 6.5 of ε_r, especially at the middle Pin.

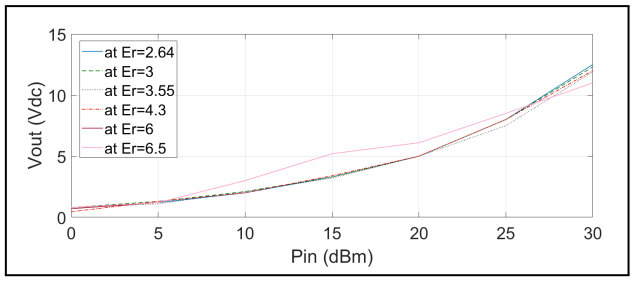

Fig. 18. Vout (V) versus Pin (dBm) of full-wave rectifier circuit for different ε_r at 2.4 GHz with LC-circuit.

Fig. 19 shows the comparison in efficiency (η) of the rectifier's performance when changes in resistance load (from 1 to 5 kΩ) are used. It has been found that the efficiency (η) decreases with an increase (R_L) in a way that is different from the case of half wave rectifier especially at low input powers.

Fig. 20 shows the comparison in efficiency (η) of the rectifier's performance when changes in diodes are made, respectively. It has been investigated that the best efficiency (η) was with the use of the HSMS2820 diode and the worst with the HSMS282C diode.

Fig. 21 shows the comparison in efficiency (η) of the rectifier's performance when changes in ε_r are made, respectively. It has been observed that an ε_r of 4.3 has fulfilled the best efficiency (η) among other values. This value of dielectric constant represents the FR-4 substrate.

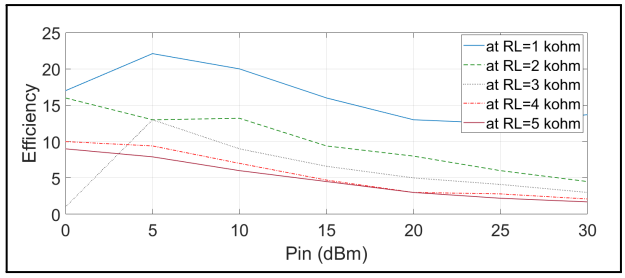

Fig. 19. Efficiency (η) versus Pin (dBm) of full-wave rectifier circuit for different values of resistance load (R_L) at 2.4 GHz with LC-circuit.

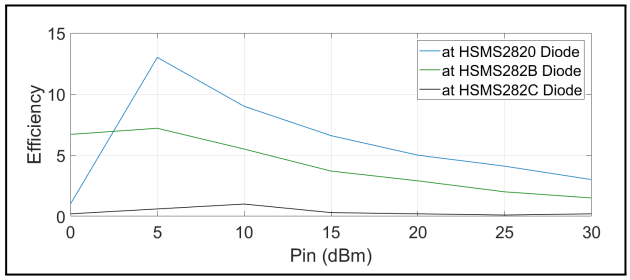

Fig. 20. Efficiency (η) versus Pin (dBm) of full-wave rectifier circuit for different Diodes at 2.4 GHz with LC-circuit.

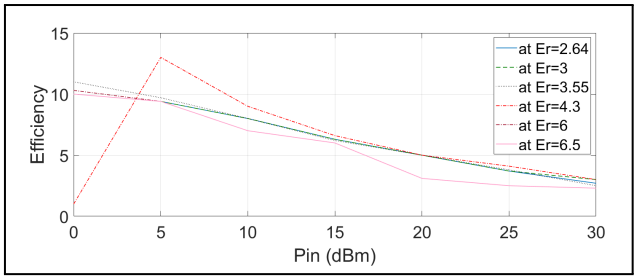

Fig. 21. Efficiency (η) versus Pin (dBm) of full-wave rectifier circuit for different ε_r at 2.4 GHz with LC-circuit.

D. Voltage Doubler rectifier circuit

Another rectifier circuit is applied by using the voltage doubler rectifier. At the input, the series capacitance acts as a voltage doubler. Additionally, the output has a capacitance to smooth the DC output before it is fed to the load as DC power or stored in a battery, as illustrated in Fig. 22. The matching network has done the job perfectly, where excellent matching is achieved, as shown in the S-parameters curve in Fig. 23.

Fig. 24 shows the comparison in Vout of the rectifier's

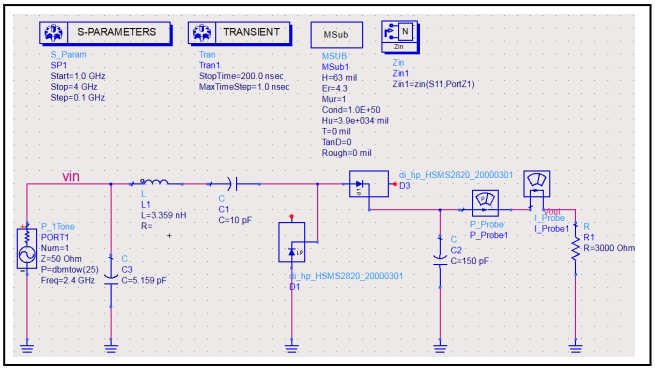

Fig. 22. Voltage doubler rectifier circuit operating at 2.4 GHz with LC-circuit.

performance when changing the resistance load (R_L) (from 1 to 5 kΩ) with a step of 1 kΩ. It is seen that the highest of Vout is at high (R_L) with huge differences at higher input power.

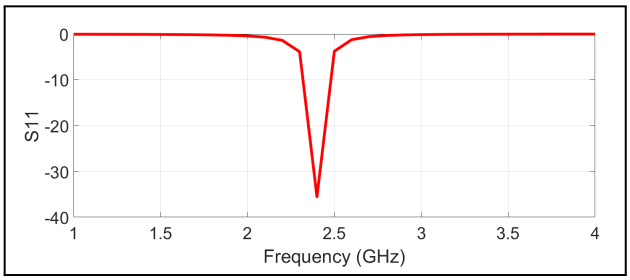

Fig. 23. Simulated S11 of voltage doubler rectifier circuit at 2.4 GHz with LC-circuit.

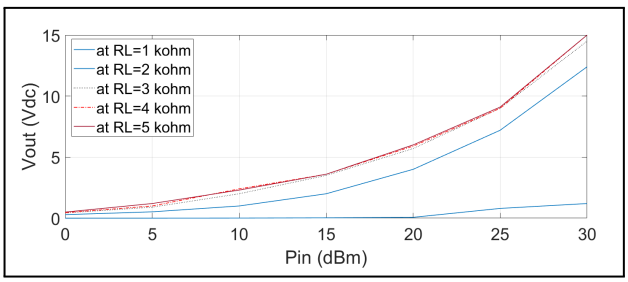

Fig. 24. Vout (V) versus Pin (dBm) of voltage doubler rectifier circuit for different values of resistance load (R_L) at 2.4 GHz with LC-circuit.

Fig. 25 shows the comparison in Vout of the rectifier's performance when changing diodes, where HSMS2820, HSMS282B, and HSMS282C diodes are employed. It has been discovered that the diode HSMS282B shows the best performance.

Fig. 26 shows the comparison in Vout of the rectifier's performance when changing in ε_r, where 2.64, 3, 3.55, 4.3, 6, and 6.5 are used. It has been noticed that the differences are almost negligible.

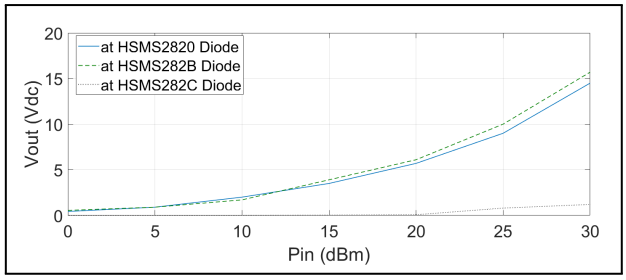

Fig. 25. Vout (V) versus Pin (dBm) of voltage doubler rectifier circuit for different Diodes at 2.4 GHz with LC-circuit.

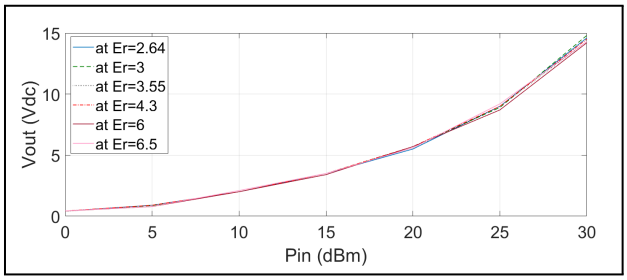

Fig. 26. Vout (V) versus Pin (dBm) of voltage doubler rectifier circuit for different ε_r at 2.4 GHz with LC-circuit.

Fig. 27 shows the comparison in efficiency (η) of the rectifier's performance when changes in resistance load (from 1 to 5 kΩ) are used. It has been found that the efficiency (η) decreases with an increase (R_L) at higher input powers.

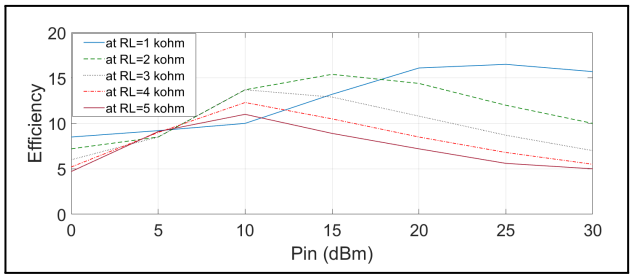

Fig. 27. Efficiency (η) versus Pin (dBm) of voltage doubler rectifier circuit for different values of resistance load (R_L) at 2.4 GHz with LC-circuit.

Fig. 28 shows the comparison in efficiency (η) of the rectifier's performance when changes in diodes are made. is found that the best efficiency (η) was with the use of the HSMS2820 diode and the worst with the HSMS282C diode.

Fig. 29 shows the comparison in efficiency (η) of the rectifier's performance when changes in ε_r are made, respec-

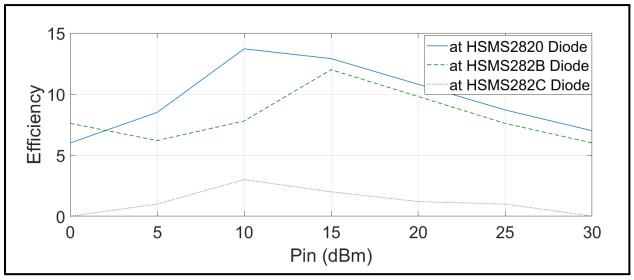

Fig. 28. Efficiency (η) versus Pin (dBm) of voltage doubler rectifier circuit for different Diodes at 2.4 GHz with LC-circuit.

tively. It is clear that the efficiency (η) almost kept the same with a different ε_r of substrate are used.

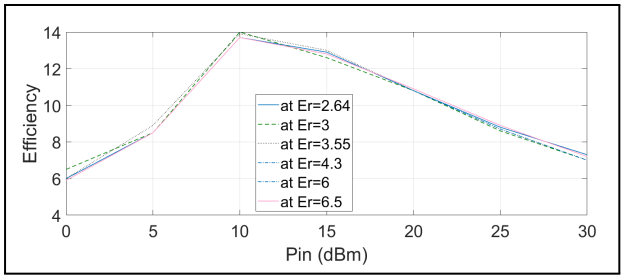

Fig. 29. Efficiency (η) versus Pin (dBm) of voltage doubler rectifier circuit for different ε_r at 2.4 GHz with LC-circuit.

E. Villard charge pump rectifier circuit

At this time, the Villard charge pump rectifier is emloyed, also known as the Villard cascade or Villard doubler. It is an electrical circuit used for rectifying and multiplying the voltage of an alternating current (AC) input signal. It was named after Paul Ulrich Villard. The Villard charge pump rectifier is a type of voltage multiplier circuit that can generate a DC voltage that is several times higher than the peak value of the AC input voltage. It is primarily used in applications where high-voltage DC is required, such as in certain types of power supplies, electrostatic generators, and X-ray machines. The basic configuration of the Villard charge pump rectifier consists of a series of diodes and capacitors connected in a cascade arrangement, as illustrated in Fig. 30. The diodes are used to rectify the AC input voltage, allowing only the positive half-cycles to pass through, while the capacitors store and accumulate charge. The output voltage is taken across the capacitors. The matching network has done the job perfectly, where excellent matching is achieved, as shown in the S-parameters curve in Fig. 31.

Fig. 32 shows the comparison in Vout of the rectifier's performance when changing the resistance load (R_L) (from

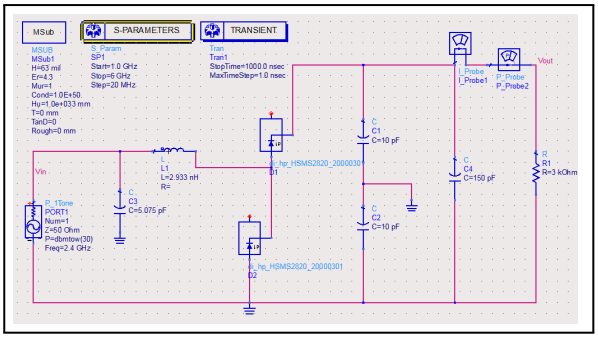

Fig. 30. Villard charge pump rectifier circuit operating at 2.4 GHz with LC-circuit.

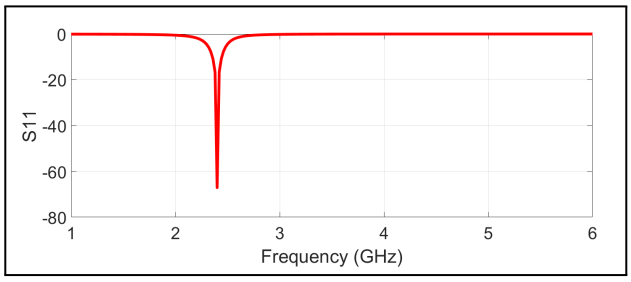

Fig. 31. Simulated S11 of Villard charge pump rectifier circuit at 2.4 GHz with LC-circuit.

1 to 5 kΩ) with a step of 1 kΩ. It has been found that there is little impact on the Vout at low input power (Pin) on the contrary at high input power (Pin).

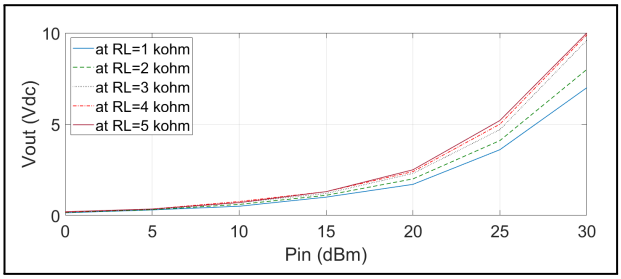

Fig. 32. Vout (V) versus Pin (dBm) of Villard charge pump rectifier circuit for different values of resistance load (R_L) at 2.4 GHz with LC-circuit.

Fig. 33 shows the comparison in Vout of the rectifier's performance when changing diodes, where HSMS2820, HSMS282B, and HSMS282C diodes are used. It has been discovered that the diode HSMS2820 outperform other types.

Fig. 34 shows the comparison in Vout of the rectifier's performance when changing in ε_r, where 2.64, 3, 3.55, 4.3, 6, and 6.5 are used. It has been concluded that the differences are negligible.

Fig. 35 shows the comparison in efficiency (η) of the

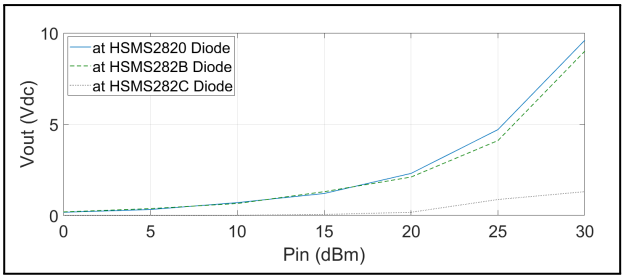

Fig. 33. Vout (V) versus Pin (dBm) of Villard charge pump rectifier circuit for different Diodes at 2.4 GHz with LC-circuit.

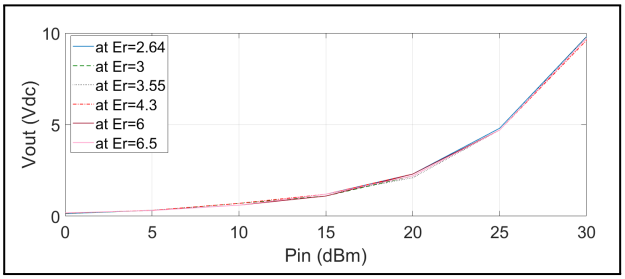

Fig. 34. Vout (V) versus Pin (dBm) of Villard charge pump rectifier circuit for different ε_r at 2.4 GHz with LC-circuit.

rectifier's performance when changing the load resistance (from 1 to 5 kΩ). It has been found that the efficiency (η) decreases when increasing (R_L), with the highest (η) at (R_L) equals to 3 kΩ at 30 dBm of Pin.

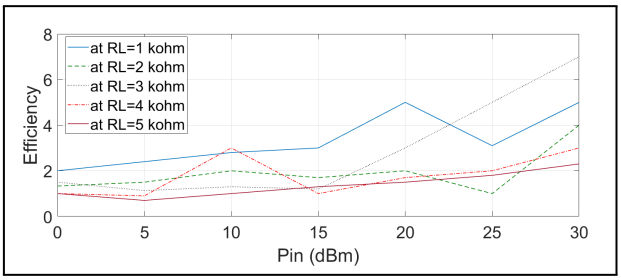

Fig. 35. Efficiency (η) versus Pin (dBm) of Villard charge pump rectifier circuit for different values of resistance load (R_L) at 2.4 GHz with LC-circuit.

Fig. 36 shows the comparison in efficiency (η) of the rectifier's performance when changes in diodes are made. It has been seen that the best efficiency (η) was with the use of the HSMS2820 diode and the worst with the HSMS282C diode especially at high input power (Pin).

Fig. 37 shows the comparison in efficiency (η) of the rectifier's performance when changes in ε_r are made. It has been noted that the efficiency (η) almost matches a different ε_r of substrate except at 4.3 especially at high input power

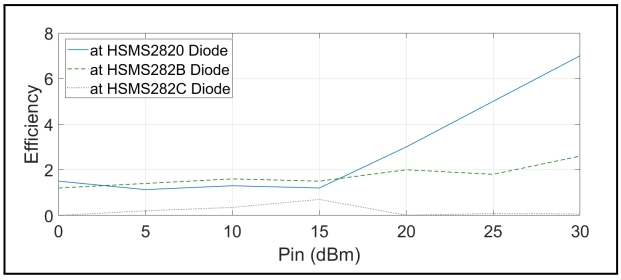

Fig. 36. Efficiency (η) versus Pin (dBm) of villard charge pump rectifier circuit for different Diodes at 2.4 GHz with LC-circuit.

(Pin).

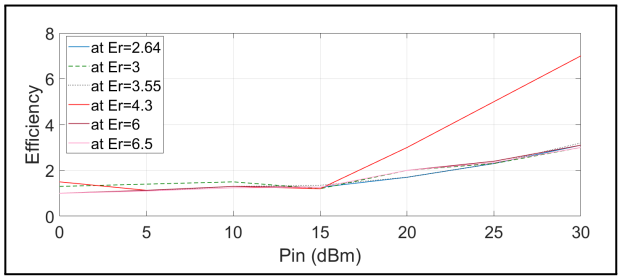

Fig. 37. Efficiency (η) versus Pin (dBm) of Villard charge pump rectifier circuit for different ε_r at 2.4 GHz with LC-circuit.

F. Graetz charge pump rectifier circuit

The Graetz charge pump, also known as a voltage doubler, is an electronic circuit used to generate a higher DC voltage from a lower DC voltage source. It is named after its inventor, Leo Graetz. The charge pump is a type of voltage multiplier circuit that utilizes diodes and capacitors to achieve voltage doubling. The basic configuration of a Graetz charge pump consists of four diodes and two capacitors arranged in a bridge-like structure, as shown in Fig. 38. The input voltage is applied across the input terminals of the charge pump circuit. During the charging phase, the capacitors are charged in parallel with the input voltage. Then, during the pumping phase, the charge stored in the capacitors is pumped to the output terminals in series, effectively doubling the voltage. The S-parameters curve is very good at 2.4 GHz, as shown in Fig. 39.

Here's a step-by-step explanation of the operation of a Graetz charge pump:

1. Charging Phase: Initially, all the diodes in the circuit are reverse-biased, preventing any current flow. During this phase, the capacitors C1 and C2 get charged to the input voltage level through the diodes D1 and D2,

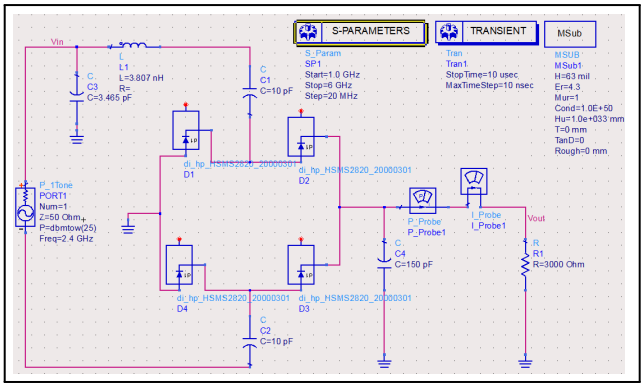

Fig. 38. Graetz charge pump rectifier circuit operating at 2.4 GHz with LC-circuit.

respectively. The voltage across each capacitor is equal to the input voltage.

2. Pumping Phase: In this phase, the input voltage is removed, and the capacitors are connected in series with the help of the diodes D3 and D4. The diodes D1 and D2 are now forward-biased, while D3 and D4 are reverse-biased. The voltage across C1 and C2 adds up, resulting in a doubled voltage at the output terminals.

3. Voltage Regulation: The output voltage of the charge pump is dependent on the capacitance values and the load connected to it. The voltage across the capacitors decreases as the charge is pumped into the load. To maintain a stable output voltage, a feedback control mechanism or regulation circuitry may be employed.

Fig. 40 shows the comparison in Vout of the rectifier's performance when changing the resistance load (R_L) (from 1 to 5 kΩ) with a step of 1 kΩ. It has been investigated that there is little impact on the Vout at low input power (Pin) on the contrary at high input power (Pin), and it is noticed that a higher Vout can be achieved at higher R_L.

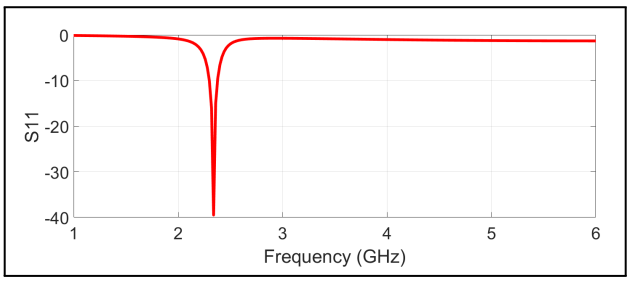

Fig. 39. Simulated S11 of Graetz charge pump rectifier circuit at 2.4 GHz with LC-circuit.

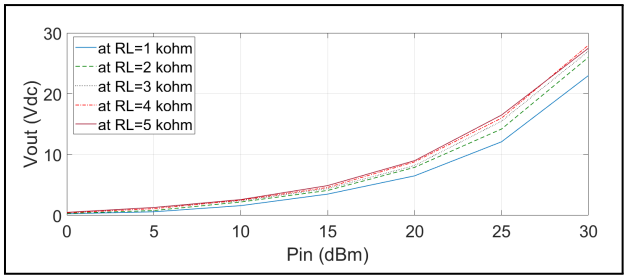

Fig. 40. Vout (V) versus Pin (dBm) of Graetz charge pump rectifier circuit for different values of resistance load (R_L) at 2.4 GHz with LC-circuit.

Fig. 41 shows the comparison in Vout of the rectifier's performance when changing diodes, where HSMS2820, HSMS282B, and HSMS282C diodes are employed. It has been discovered that the differences are almost negligible when changing the diodes for this type of rectifiers.

Fig. 42 shows the comparison in Vout of the rectifier's performance when changing in ε_r, where 2.64, 3, 3.55, 4.3, 6, and 6.5 are utilized. It has been obvious that the differences are almost negligible, except in the middle of Pin where there is a slight difference noticed.

Fig. 43 shows the comparison in efficiency (η) of the rectifier's performance when changing load resistance (from 1 to 5 kΩ). It has been found that the efficiency (η) decreases with an increase (R_L), with the highest (η) at (R_L) equal to 1 kΩ at 30 dBm of Pin, where the η =50%.

Fig. 44 shows the comparison in efficiency (η) of the rectifier's performance when changes in diodes are made, respectively. It has been investigated that the best efficiency (η) was with the use of the HSMS282B diode and the worst with the HSMS2820 diode especially at low input power (Pin).

Fig. 45 shows the comparison in efficiency (η) of the rectifier's performance when changes in ε_r are made. It has been clear that the efficiency (η) almost unchanged at different ε_r of substrate.

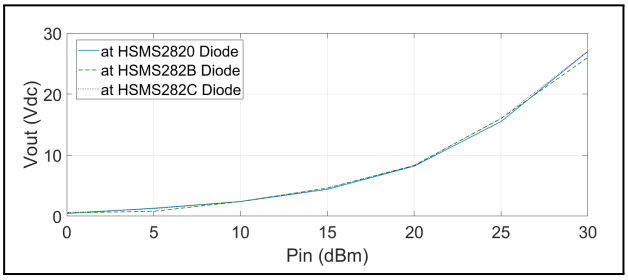

Fig. 41. Vout (V) versus Pin (dBm) of Graetz charge pump rectifier circuit for different Diodes at 2.4 GHz with LC-circuit.

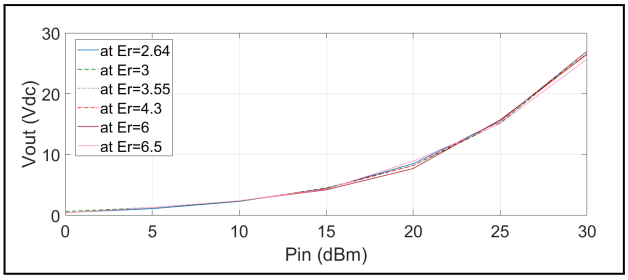

Fig. 42. Vout (V) versus Pin (dBm) of Graetz charge pump rectifier circuit for different ε_r at 2.4 GHz with LC-circuit.

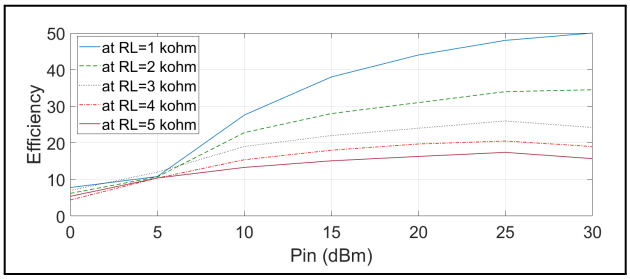

Fig. 43. Efficiency (η) versus Pin (dBm) of Graetz charge pump rectifier circuit for different values of resistance load (R_L) at 2.4 GHz with LC-circuit.

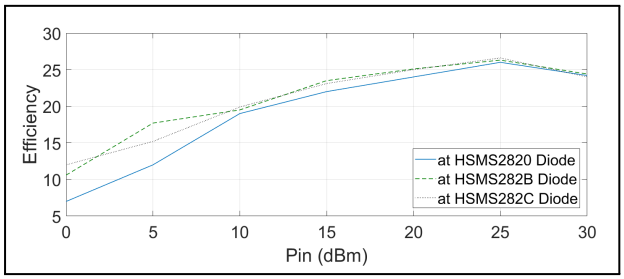

Fig. 44. Efficiency (η) versus Pin (dBm) of Graetz charge pump rectifier circuit for different Diodes at 2.4 GHz with LC-circuit.

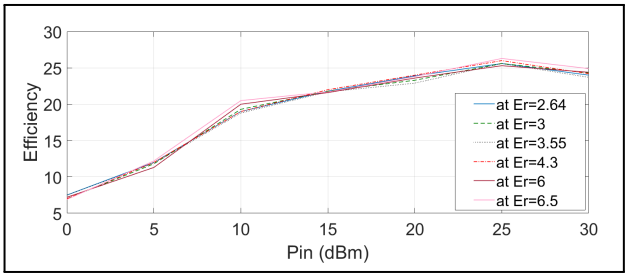

Fig. 45. Efficiency (η) versus Pin (dBm) of Graetz charge pump rectifier circuit for different ε_r at 2.4 GHz with LC-circuit.

G. Dickson charge pump rectifier circuit

The Dickson charge pump rectifier is another type of voltage multiplier circuit that is commonly used to generate a higher DC voltage from a lower AC voltage source. It is named after its inventor, J. M. Dickson. The Dickson charge pump rectifier is particularly useful in applications where a higher voltage is needed, such as in power management circuits and low-power electronics. The Dickson charge pump rectifier is based on the concept of cascading multiple stages of diode-capacitor voltage doublers. Each stage consists of a diode and a capacitor connected in series. The output of one stage is connected to the input of the next stage, creating a cascaded arrangement, as shown in Fig. 46. One advantage of the Dickson charge pump rectifier is its scalability; by cascading multiple stages, the voltage multiplication factor can be increased. However, it's important to note that as the number of stages increases, the voltage drop across each diode also increases, leading to higher losses and decreased efficiency. The S11-Parameters curve is excellent at 2.4 GHz, as shown in Fig. 47.

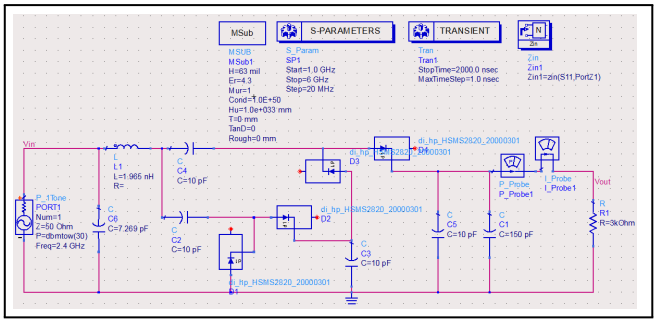

Fig. 46. Dickson charge pump rectifier circuit operating at 2.4 GHz with LC-circuit.

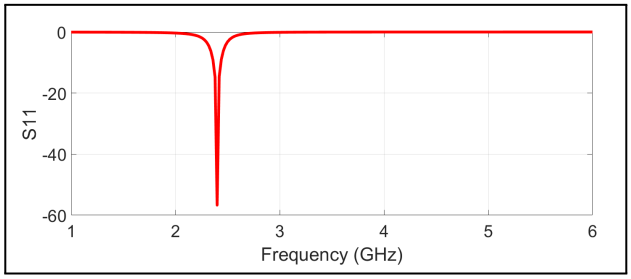

Fig. 47. Simulated S11 of Dickson charge pump rectifier circuit at 2.4 GHz with LC-circuit.

Fig. 48 shows the comparison in Vout of the rectifier's performance when changing the resistance load (R_L) (from 1 to 5 kΩ) with a step of 1 kΩ. It has been noticed that there is little impact on the Vout at low input power (Pin) while the impact is higher at higher input power (Pin), and a better Vout at higher R_L.

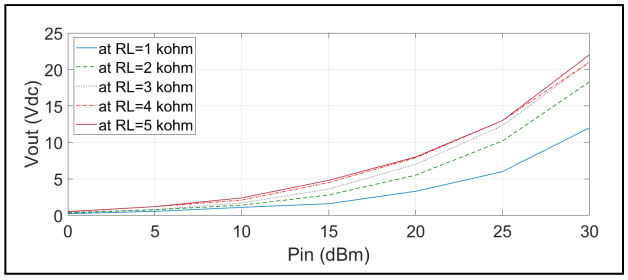

Fig. 48. Vout (V) versus Pin (dBm) of Dickson charge pump rectifier circuit for different values of resistance load (R_L) at 2.4 GHz with LC-circuit.

Fig. 49 shows the comparison in Vout of the rectifier's performance when changing diodes, where HSMS2820, HSMS282B, and HSMS282C diodes are used. It has been discovered that the diodes HSMS2820 and HSMS282B have similar performance while HSMS282C showed a very poor performance at this type of rectifiers.

Fig. 50 shows the comparison in Vout of the rectifier's performance when changing in ε_r, where 2.64, 3, 3.55, 4.3, 6, and 6.5 are used. It has been seen that the differences are almost negligible, except in the high of Pin where there is a trivial difference.

Fig. 51 shows the comparison in efficiency (η) of the rectifier's performance when changes in resistance load (from 1 to 5 kΩ) are employed. It has been found that the efficiency (η) decreases at both sides (low and high) of Pin, except the highest (η) is achieved at (R_L) equals to 2 kΩ at 30 dBm of Pin, where the recorded value is η =16%.

Fig. 52 shows the comparison in efficiency (η) of the rectifier's performance when changes in diodes are made. It has been investigated that the best efficiency (η) was with the use of the HSMS2820 diode and the worst with the HSMS282C diode.

Fig. 53 shows the comparison in efficiency (η) of the rectifier's performance when changes in ε_r are made. It has been investigated that the efficiency (η) almost differs by a different ε_r of substrate.

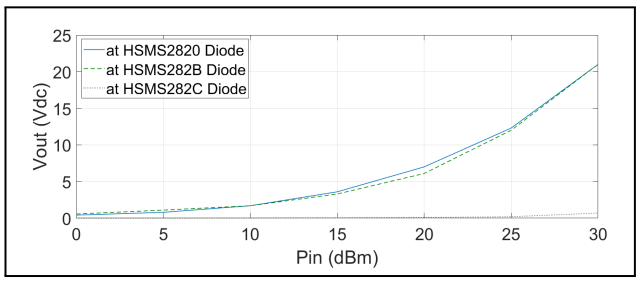

Fig. 49. Vout (V) versus Pin (dBm) of Dickson charge pump rectifier circuit for different Diodes at 2.4 GHz with LC-circuit.

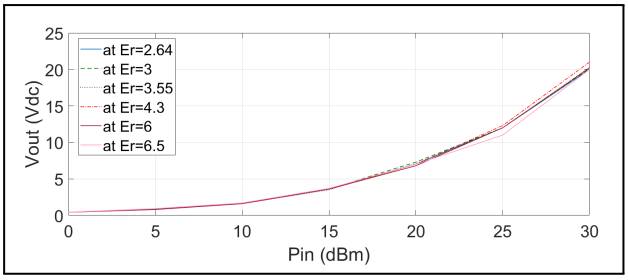

Fig. 50. Vout (V) versus Pin (dBm) of Dickson charge pump rectifier circuit for different ε_r at 2.4 GHz with LC-circuit.

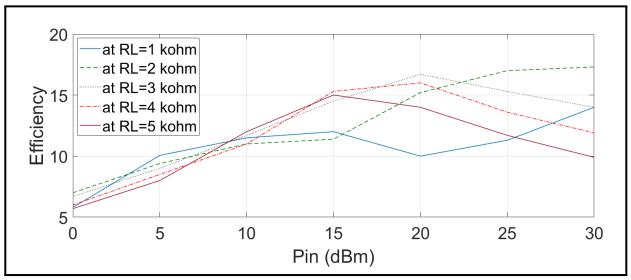

Fig. 51. Efficiency (η) versus Pin (dBm) of Dickson charge pump rectifier circuit for different values of resistance load (R_L) at 2.4 GHz with LC-circuit.

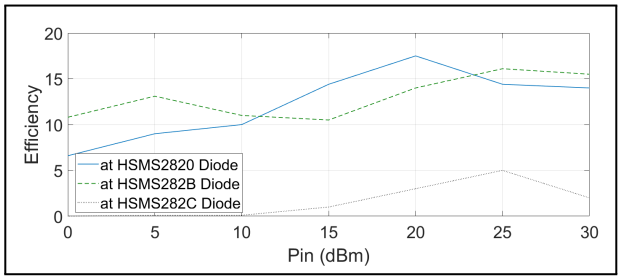

Fig. 52. Efficiency (η) versus Pin (dBm) of Dickson charge pump rectifier circuit for different Diodes at 2.4 GHz with LC-circuit.

Fig. 54 shows the comparison in Vout of the rectifier circuits performance at the resistance load (3 k Ω), HSMS2820 diode, and ε_r equal to 4.3. It has been investigated that the highest Vout with the Graetz charge rectifier circuit is about 27 V.

Fig. 55 shows the comparison in Efficiency (η) of the rectifier circuits performance at the resistance load (3 kΩ), HSMS2820 diode, and ε_r equal to 4.3. It has been found that the highest η with the Graetz charge rectifier circuit is about 27%.

Table (I) demonstrates the efficiency of different rectifier

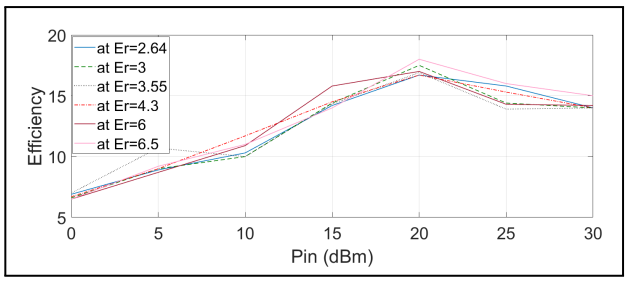

Fig. 53. Efficiency (η) versus Pin (dBm) of Dickson charge pump rectifier circuit for different ε_r at 2.4 GHz with LC-circuit.

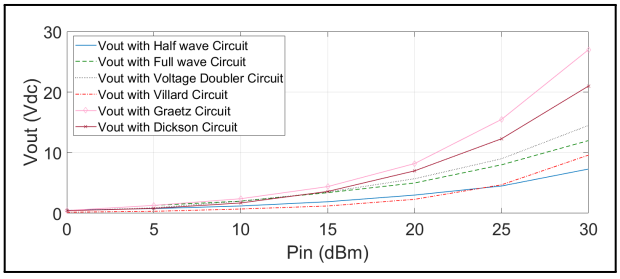

Fig. 54. Vout (V) versus Pin (dBm) of different rectifier circuits at 2.4 GHz with LC-circuit.

circuits at 10 and 30 dBm of input power (Pin) and it is found that the highest efficiency among them at input power of 10 and 30 dBm was when using the Graetz charge pump rectifier circuit.

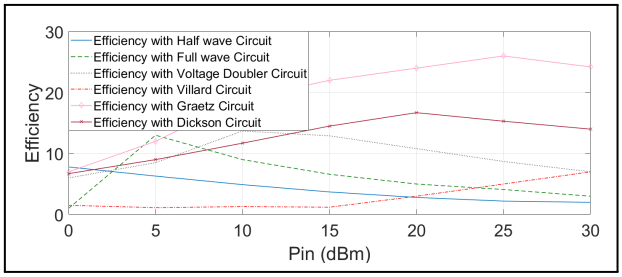

Fig. 55. Efficiency (η) versus Pin (dBm) of different rectifier circuits at 2.4 GHz with LC-circuit.

TABLE I. Show the Efficiency (η) for different Rectifier circuits at 10 and 30 dBm of input power (Pin).

Rectifier circuits	Efficiencies (η) at Pin= 10 dBm	Efficiencies (η) at Pin= 30 dBm
Graetz charge pump	19%	24%
Voltage doubler	13%	7%
Dickson charge pump	12%	14%
Full-wave	9%	3%
Half-wave	5%	%2
Villard charge pump	1%	7%

TABLE II. Show the Efficiency (η) for different Rectifier circuits at 10 and 30 dBm of input power (Pin).

Ref. /Year	Freq. (GHz)	Rectifier element & topology	PCE (%)
[24] 2020	2.45	two stage differential cross-connected (CC) rectifier	46
[25] 2018	2.5	triple band differential rectifier/Villard voltage doubler	31
[26] 2020	2.45	HSMS2852, Voltage doubler	20
[27] 2017	2.45	SMS7630, Shunt	57
[28] 2015	2.45	HSMS285, One port voltage doubler	40.5
[29] 2016	2.4	class-E rectifier circuit / Voltage multiplier technique	30
this work 2024	2.4	HSMS2820, Graetz charge pump	27

Conflict of Interest

The authors have no conflict of relevant interest to this article.

References

[1] A. Costanzo and D. Masotti, "Energizing 5g: Near-and far-field wireless energy and data trantransfer as an enabling technology for the 5g iot," *IEEE Microwave Magazine*, vol. 18, no. 3, pp. 125–136, 2017.

[2] M. Wagih, G. S. Hilton, A. S. Weddell, and S. Beeby, "Broadband millimeter-wave textile-based flexible rectenna for wearable energy harvesting," *IEEE Transactions on Microwave Theory and Techniques*, vol. 68, no. 11, pp. 4960–4972, 2020.

[3] X. Yue, M. Kauer, M. Bellanger, O. Beard, M. Brownlow, D. Gibson, C. Clark, C. MacGregor, and S. Song, "Development of an indoor photovoltaic energy harvesting module for autonomous sensors in building air quality applications," *IEEE Internet of Things Journal*, vol. 4, no. 6, pp. 2092–2103, 2017.

[4] M. A. Halimi, T. Khan, D. Surender, N. Nasimuddin, and S. Rengarajan, "Dielectric resonator antennas for rf energy-harvesting/wireless power transmission applications: A state-of-the-art review," *IEEE Antennas and Propagation Magazine*, vol. 66, no. 1, pp. 34–45, 2023.

[5] U. Olgun, C.-C. Chen, and J. L. Volakis, "Investigation of rectenna array configurations for enhanced rf power harvesting," *IEEE antennas and wireless propagation letters*, vol. 10, pp. 262–265, 2011.

[6] H. Sun, Y.-x. Guo, M. He, and Z. Zhong, "Design of a high-efficiency 2.45-ghz rectenna for low-input-power energy harvesting," *IEEE Antennas and Wireless Propagation Letters*, vol. 11, pp. 929–932, 2012.

[7] D. Surender, T. Khan, F. A. Talukdar, and Y. M. Antar, "Rectenna design and development strategies for wireless applications: A review," *IEEE Antennas and Propagation Magazine*, vol. 64, no. 5, pp. 16–29, 2021.

[8] M. A. Halimi, T. Khan, A. A. Kishk, Y. M. Antar, *et al.*, "Rectifier circuits for rf energy harvesting and wireless power transfer applications: A comprehensive review based on operating conditions," *IEEE Microwave Magazine*, vol. 24, no. 1, pp. 46–61, 2022.

[9] R. Hesham, A. Soltan, and A. Madian, "Energy harvesting schemes for wearable devices," *AEU-International Journal of Electronics and Communications*, vol. 138, p. 153888, 2021.

[10] D. Surender, M. A. Halimi, T. Khan, F. A. Talukdar, S. R. Rengarajan, *et al.*, "5g/millimeter-wave rectenna systems for radio-frequency energy harvesting/wireless power transmission applications: An overview," *IEEE Antennas and Propagation Magazine*, vol. 65, no. 3, pp. 57–76, 2022.

[11] Y. Shi, J. Jing, Y. Fan, L. Yang, Y. Li, and M. Wang, "A novel compact broadband rectenna for ambient rf energy harvesting," *AEU-International Journal of Electronics and Communications*, vol. 95, pp. 264–270, 2018.

[12] N. Shafiee, S. Tewari, B. Calhoun, and A. Shrivastava, "Infrastructure circuits for lifetime improvement of ultra-low power iot devices," *IEEE Transactions on Circuits and Systems I: Regular Papers*, vol. 64, no. 9, pp. 2598–2610, 2017.

[13] A. Roy, A. Klinefelter, F. B. Yahya, X. Chen, L. P. Gonzalez-Guerrero, C. J. Lukas, D. A. Kamakshi, J. Boley, K. Craig, M. Faisal, *et al.*, "A 6.45μw self-powered soc with integrated energy-harvesting power management and ulp asymmetric radios for portable biomedical systems," *IEEE Transactions on biomedical circuits and systems*, vol. 9, no. 6, pp. 862–874, 2015.

[14] Y. Zhang, F. Zhang, Y. Shakhsheer, J. D. Silver, A. Klinefelter, M. Nagaraju, J. Boley, J. Pandey, A. Shrivastava, E. J. Carlson, *et al.*, "A batteryless 19μw mics/ism-band energy harvesting body sensor node soc for exg applications," *IEEE Journal of solid-state circuits*, vol. 48, no. 1, pp. 199–213, 2012.

[15] Y.-P. Chen, D. Jeon, Y. Lee, Y. Kim, Z. Foo, I. Lee, N. B. Langhals, G. Kruger, H. Oral, O. Berenfeld, *et al.*, "An injectable 64 nw ecg mixed-signal soc in 65 nm for arrhythmia monitoring," *IEEE Journal of Solid-State Circuits*, vol. 50, no. 1, pp. 375–390, 2014.

[16] P. Saffari, A. Basaligheh, and K. Moez, "An rf-to-dc rectifier with high efficiency over wide input power range for rf energy harvesting applications," *IEEE Transactions on Circuits and Systems I: Regular Papers*, vol. 66, no. 12, pp. 4862–4875, 2019.

[17] M. A. Karami and K. Moez, "Systematic co-design of matching networks and rectifiers for cmos radio frequency energy harvesters," *IEEE Transactions on Circuits and Systems I: Regular Papers*, vol. 66, no. 8, pp. 3238–3251, 2019.

[18] P. Xu, D. Flandre, and D. Bol, "Analysis, modeling, and design of a 2.45-ghz rf energy harvester for swipt iot smart sensors," *IEEE Journal of Solid-State Circuits*, vol. 54, no. 10, pp. 2717–2729, 2019.

[19] A. Khalifa, Y. Liu, Y. Karimi, Q. Wang, A. Eisape, M. Stanaćević, N. Thakor, Z. Bao, and R. Etienne-Cummings, "The microbead: A 0.009 mm 3 implantable wireless neural stimulator," *IEEE transactions on biomedical circuits and systems*, vol. 13, no. 5, pp. 971–985, 2019.

[20] F. Laiwalla, J. Lee, A.-H. Lee, E. Mok, V. Leung, S. Shellhammer, Y.-K. Song, L. Larson, and A. Nurmikko, "A distributed wireless network of implantable sub-mm cortical microstimulators for brain-computer interfaces," in *2019 41st Annual International Conference of the IEEE Engineering in Medicine and Biology Society (EMBC)*, pp. 6876–6879, IEEE, 2019.

[21] Y. Zhao, R. L. Rennaker, C. Hutchens, and T. S. Ibrahim, "Implanted miniaturized antenna for brain computer interface applications: analysis and design," *PloS one*, vol. 9, no. 7, p. e103945, 2014.

[22] K.-W. Yang, K. Oh, and S. Ha, "Challenges in scaling down of free-floating implantable neural interfaces to millimeter scale," *IEEE Access*, vol. 8, pp. 133295–133320, 2020.

[23] R. Sobot, *Wireless Communication Electronics*. Springer, 2020.

[24] X. Li, Y. Lu, M. Huang, and R. P. Martins, "A 2.4-ghz mid-field cmos wireless power receiver achieving 46% maximum pce and 163-mw output power," *IEEE Transactions on Circuits and Systems II: Express Briefs*, vol. 67, no. 2, pp. 360–364, 2019.

[25] S. Chandravanshi, S. S. Sarma, and M. J. Akhtar, "Design of triple band differential rectenna for rf energy harvesting," *IEEE Transactions on Antennas and Propagation*, vol. 66, no. 6, pp. 2716–2726, 2018.

[26] M. Koohestani, J. Tissier, and M. Latrach, "A miniaturized printed rectenna for wireless rf energy harvesting around 2.45 ghz," *AEU-International Journal of Electronics and Communications*, vol. 127, p. 153478, 2020.

[27] J. Costantine, A. Eid, M. Abdallah, Y. Tawk, and A. Ramadan, "A load independent tapered rf harvester," *IEEE Microwave and Wireless Components Letters*, vol. 27, no. 10, pp. 933–935, 2017.

[28] J. Kimionis, M. Isakov, B. S. Koh, A. Georgiadis, and M. M. Tentzeris, "3d-printed origami packaging with inkjet-printed antennas for rf harvesting sensors," *IEEE Transactions on Microwave Theory and Techniques*, vol. 63, no. 12, pp. 4521–4532, 2015.

[29] S. Dehghani and T. Johnson, "A 2.4-ghz cmos class-e synchronous rectifier," *IEEE Transactions on Microwave theory and techniques*, vol. 64, no. 5, pp. 1655–1666, 2016.